PROCEEDINGS OF SPIE

SPIEDigitalLibrary.org/conference-proceedings-of-spie

Adaptive delay lines implemented on a photonics chip for extended-range, high-speed absolute distance measurement

C. Coggrave, P. Ruiz, J. Huntley, C. Nolan, A. Gribble, et al.

C. R. Coggrave, P. D. Ruiz, J. M. Huntley, C. E. Nolan, A. P. Gribble, H. Du, M. Banakar, X. Yan, D. T. Tran, C. G. Littlejohns, "Adaptive delay lines implemented on a photonics chip for extended-range, high-speed absolute distance measurement," Proc. SPIE 12334, Emerging Applications in Silicon Photonics III, 1233406 (11 January 2023); doi: 10.1117/12.2647526

SPIE.

Event: SPIE Photonex, 2022, Birmingham, United Kingdom

Downloaded From: https://www.spiedigitallibrary.org/conference-proceedings-of-spie on 08 Sep 2023 Terms of Use: https://www.spiedigitallibrary.org/terms-of-use

Adaptive delay lines implemented on a photonics chip for extended-range, high-speed absolute distance measurement

C. R. Coggrave[a]*, P. D. Ruiz[a], J. M. Huntley[a], C. E. Nolan[a], A. P. Gribble[b], H. Du[c], M. Banakar[c], X. Yan[c], D. T. Tran[c], and C. G. Littlejohns[c]

[a]Loughborough University, Wolfson School of Mechanical, Electrical and Manufacturing Engineering, Loughborough, LE11 3TU, UK; [b]Renishaw PLC, New Mills, Wotton-under-Edge, GL12 8JR, UK; [c]University of Southampton, Optoelectronics Research Centre, Southampton, SO17 1BJ, UK

*c.r.coggrave@lboro.ac.uk

ABSTRACT

High-speed (upwards of 10^5 coordinates s^{-1}) and long-range (~10 m) absolute distance measurement applications based on frequency scanning interferometry (FSI) generate very high modulation frequencies (typically >100 GHz) due to the laser frequency sweep rate and the large imbalance between the reference and object arms. Such systems are currently impractical due to the extremely high cost associated with sampling at these signal frequencies. Adaptive delay lines (ADLs) were recently proposed as a solution to balance the interferometer and therefore reduce sampling rate requirements by a factor of 2^N, where N is the number of switches in the ADL [1, 2]. The technique has been successfully demonstrated in the lab using bulk optics and optical fiber configurations, and further reduction in size and cost will increase the breadth of metrology applications that can be addressed. Silicon photonics constitute an effective platform to miniaturize ADLs to chip-scale, simplifying instrument manufacture and providing a more robust configuration compared to bulk-optics and fiber-based solutions. We discuss the design and fabrication of chip-scale ADLs on a silicon on insulator (SOI) photonics platform, using optical switches based on heaters, multi-mode interferometer (MMI) couplers and Mach-Zehnder interferometers (MZI). We also establish the heater voltages of 4 switches in series, required to switch the optical path in the reference arm, a necessary step to use the device for FSI range measurements.

Keywords: Frequency scanning interferometry, FSI, FMCW, lidar, absolute distance measurement, photonics, adaptive delay lines

1. INTRODUCTION

Frequency scanning interferometry (FSI), also known as frequency modulated continuous wave lidar (FMCW), is nowadays an established technique for absolute distance measurements [1-4]. It can be implemented in single-point, raster-scanning and diverging beam configurations, and incorporated into laser trackers. The main advantage of FSI vs. fringe counting (or differential) interferometers is that blocking the beam does not require homing a retroreflector and moving it back to the target position while maintaining line of sight to keep track of the fringe order. Applications range from measuring dimensional changes in the ATLAS detector in the Large Hadron Collider [5], to shape measurement [6, 7] and displacement and target velocity measurements [1, 2, 8, 9]. By incorporating gas cells, the range estimate can be made traceable to standards [10]. FSI involves a tunable laser and an interferometer that splits the beam into an object and a reference arm, and then combines the light returning from a target (the object wave) with a local reference wave. Their interference signal has a frequency proportional to Λ and f_s, the optical path difference (OPD) between the two waves, and the laser scan repetition rate, respectively. For a linear frequency ramp and a non-dispersive medium $f = \Lambda f_s \Delta\lambda/\lambda_c^2$ [1, 2] with $\Delta\lambda$ the tuning range and λ_c the centre wavelength. State-of-the-art tunable laser sources such as VCSELs and FDML lasers can produce scan rates of 100s of kHz to several MHz, respectively, combined with $\Delta\lambda$ values exceeding 100 nm at λ_c = 1.0, 1.3 or 1.5 µm. These characteristics enable high-accuracy long-range distance measurement at rates in the range 10^5–10^6 s^{-1} [2], thus offering significant potential for dimensional quality control at rates 2-3 orders of magnitude higher than current commercial FSI-based instruments. However, there are significant challenges that need to be overcome. For example, with $\Delta\lambda$ = 100 nm, λ_c = 1.3 µm, f_s = 100 kHz, the interference signal $f \sim 12$ GHz at a distance $z \sim 1$ m ($\Lambda = 2z \sim 2$ m for coaxial illumination and observation directions), and proportionally higher for a 10 m range, requiring

Emerging Applications in Silicon Photonics III, edited by Callum G. Littlejohns, Marc Sorel,
Proc. of SPIE Vol. 12334, 1233406 · © 2023 SPIE · 0277-786X
doi: 10.1117/12.2647526

Downloaded From: https://www.spiedigitallibrary.org/conference-proceedings-of-spie on 08 Sep 2023
Terms of Use: https://www.spiedigitallibrary.org/terms-of-use

fast photodetectors and DAQ hardware with extremely high sampling rates greater than 100 GS s^{-1} (typical digital storage scopes with 70 GHz bandwidth, single channel and 200 GS s−1 cost over $300k). Real time processing of such high-speed data streams is non-trivial. Moreover, the coherence length of these laser sources is not well characterized and may pose limitations for long Λ. Finally, Fourier domain peak broadening and splitting due to non-linear frequency sweeps increase in severity with increasing Λ. To solve these problems, the concept of adaptive delay lines (ADL) was proposed [1, 2]. The ADL is introduced into the reference arm of the interferometer and can reduce Λ to the point at which the modulation frequency drops to levels that can be dealt with by standard photodetectors and DAQs (∼ 1 GS s^{-1}) whilst simultaneously reducing data throughput, removing the need for a long coherence length source, and reducing Fourier domain peak broadening effects. The ADL principle is illustrated schematically in Fig. 1(b), where the reference beam passes through $N = 3$ optical switches S_0, S_1, S_2 in series. Each switch, which may be mechanically, optically or electronically controlled, selects one of two optical paths via an imbalanced MZI to the next switch: the path indicated with a solid line. The last two paths are recombined at the coupler (CPL) and the length-adjusted reference beam interferes with the object wave. If the MZIs have exponentially increasing lengths $d_0, 2d_0, \ldots\ 2^{N-1}d_0$, then by controlling the state of the switches the total delay can be selected in steps of d_0 within the range 0 to $(2^N-1)d_0$. A proof-of-principle ADL based on polarization optics (with the switches implemented using half-wave-plates and polarizing beam splitters) was demonstrated in [1] and extended in [2] using a VCSEL tunable laser at 10^5 sweeps per second. Range, displacement, and velocity were determined from the phase of the interference signal, achieving sub-nanometer displacement resolution, sub-100-nm range resolution, and velocity resolution of 12 μm s−1 over a range of 300 mm.

In this paper, we implemented a 4-switch active ADL on a SOI photonic integrated circuit (PIC), see Fig. 2. The MZIs have nominal optical path delays of 4, 8, 16 and 32 mm, enabling a path balancing of up to 60 mm in air to demonstrate the principle of actively switched ADLs. Each switch consists of an MMI splitter, an MZI with a heater (thin gold wire) on top of the rib waveguide that forms one of the MZI optical paths, and an MMI combiner. By driving a current through the heater with an external D/A board connectorized to the PIC via an array of micro-electrodes, a phase shift is introduced (due to the thermo-optic effect and material thermal expansion) that determines the intensity ratio at the output 2×2 MMI coupler in the MZI. In section 2 we describe the PIC design and fabrication, in section 3 the methodology followed to identify the voltages required by each switch to route the optical path through the short and long arms in their corresponding MZI, and in section 4 the challenges that we encountered and future steps to integrate the active ADL in an FSI setup for a range measurement demonstrator.

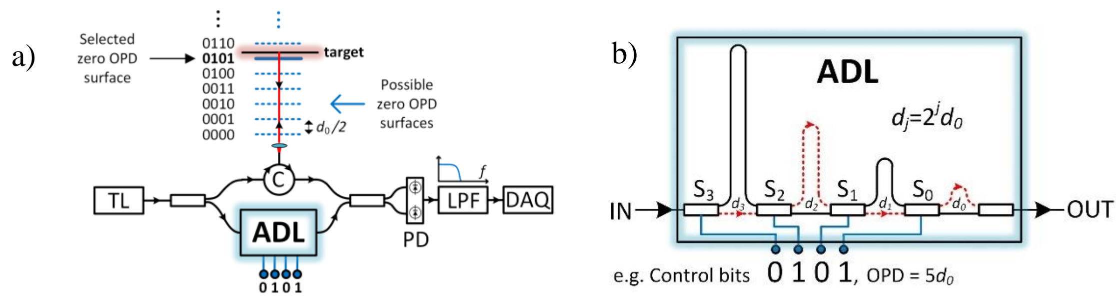

Figure 1: a) Frequency scanning interferometer with an active adaptive delay line in the reference arm (TL: tunable laser, C: circulator, PD: balanced photodetector, LPF: low-pass filter and DAQ: data acquisition board). The bit configuration that drives the ADL effectively locates the datum (zero OPD between object and reference beam) along the measurement arm. The goal is to use the datum that is closest to the target, to reduce the frequency of the interference signal. For example, bit configuration `0101` adds an optical path of $5d_0$ to the reference beam and produces a low frequency signal when it interferes with the object beam. b) Schematic view of an ADL with 4 Mach-Zehnder interferometers in series, with exponentially increasing imbalance and connected with switches S_0, S_1, S_2 and S_3. Couper CPL recombines the complex amplitude at the output of the last MZI.

2. PIC DESIGN AND FABRICATION

The devices were fabricated using the open source, license free CORNERSTONE platform, which can be accessed directly [11] or via EUROPRACTICE [12]. The devices were built in the standard multi-project-wafer (MPW) 220 nm silicon-on-insulator platform consisting of a 220 nm thick Si overlayer and a 2 µm thick buried oxide layer (BOX). Light is coupled into and out of the photonic integrated circuit (PIC) via grating couplers formed via a 70 nm partially etched Si

Downloaded From: https://www.spiedigitallibrary.org/conference-proceedings-of-spie on 08 Sep 2023
Terms of Use: https://www.spiedigitallibrary.org/terms-of-use

layer or via an edge coupler formed in a strip waveguide by cleaving the chip facet. Strip waveguides were formed to route and manipulate the light by fully etching the Si layer. Both Si etching steps were performed using an inductively coupled plasma (ICP) etch process based on the gases SF_6 and C_4F_8. After waveguide and grating coupler formation, a 1 µm SiO_2 top cladding layer was deposited by plasma enhanced chemical vapor deposition (PECVD), followed by a heater fabrication process for thermal phase shifters. The heater process comprises two metal lift-off steps, firstly a TiN based filament layer, and secondly a Ti and Au contact pad layer. All lithography steps were carried out on the 200 mm wafer-scale by 248 nm deep-UV projection lithography. After all fabrication steps were complete, the wafer was diced into 11.3×7.5 mm^2 die.

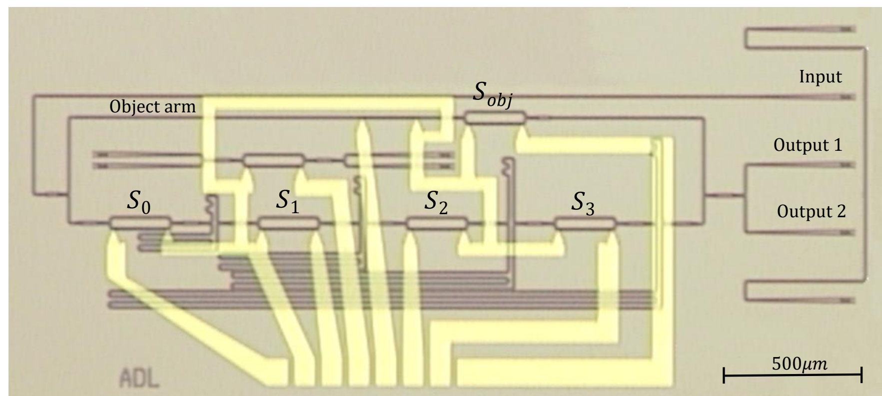

Figure 2: Proof-of-principle active ADL on a SOI photonic integrated circuit. The top arm of the high-level Mach-Zehnder interferometer between splitters 1 and 2 represents the object beam, while the lower arm consists of 4-switch active ADL, with 4 exponentially increasing path lengths of 1, 2, 4 and 8 mm that, given a group index n_g = 4.351 (determined experimentally on the PIC), correspond to ~ 4.35, 8.70, 17.40 and 34.81 mm in air. The object beam has an extra pair of heaters for phase and intensity ratio control of the main interferometer. The vertical separation between successive grating couplers on the right-hand side of the figure is 250 µm.

3. CALIBRATION OF OPTICAL SWITCHES IN SERIES

To control the ADL, each switch must be calibrated to identify the voltages V_{i1} and V_{i0} that route light through the long and short paths, respectively, of the MZI immediately downstream, with $i = 0, 1, 2, 3$ the switch index. This task is straightforward for a single switch: using a fixed wavelength in the input port/s a voltage ramp is applied to the heater and the intensity at both outputs is recorded, from which the phase vs. voltage function can be established. The voltages V_{i1} and V_{i0} that produce a maximum (minimum) intensity in the long (short) arm of the MZI and a corresponding minimum (maximum) in the other, are identified and used thereafter to control the routing of light through the switch.

When several switches are connected in series, this calibration is not as simple, as we only have access to the intensity at the main output of the interferometer. As each switch can route light along waveguides of exponentially increasing lengths, the analysis can be done in the frequency domain. Using a tunable laser, the input is swept over several tens of nm and the interferometer signal is recorded (with or without the simulated object beam which is activated via control of an extra switch S_{obj} that controls the object/reference beam intensity ratio between object and reference beams to improve signal modulation). The optical outputs shown in Fig. 2 are measured using a balanced photodiode (PD) which generates differential voltage V_{PD}. The Fourier transform of the signal V_{PD} reveals different peaks that correspond to light passing through paths of different lengths. By changing the voltages applied to the heaters, some peaks appear and disappear, and the task consists in finding V_{i1} and V_{i0} that activate the different delays in the ADL.

Figure 3 shows the peaks obtained for all $V_i = 0$, after signal linearization to eliminate non-linearities in the frequency scan of the laser (Santec TSL-510 type A). These peaks correspond to the interference between the simulated object arm in the high-level MZI in Fig. 2 and the reference arm with the ADL (cross-correlation terms), but the calibration can also be performed with the auto-correlation terms, i.e. when no object beam is present. Secondary peaks also appear that may be due to spurious Fabry-Perot effects in the interferometer.

Downloaded From: https://www.spiedigitallibrary.org/conference-proceedings-of-spie on 08 Sep 2023
Terms of Use: https://www.spiedigitallibrary.org/terms-of-use

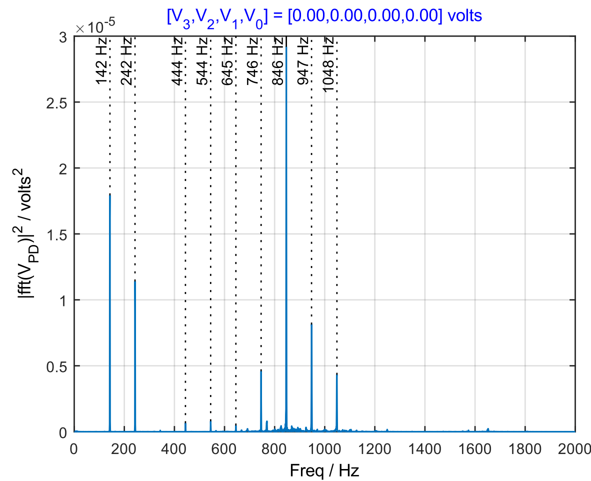

Figure 3: Frequency response observed with no voltage applied across the heaters. Peaks in the frequency domain correspond to the optical path differences between the object beam and multiple delays in the ADL. In principle, up to 16 dominant peaks corresponding to all $2^N = 16$ possible delays in a 4-switch ADL may be present.

4. DISCUSSION AND CONCLUSIONS

Calibration to determine the ADL switch voltages V_{i1} and V_{i0} for $i = 0, 1, 2, 3$ can be performed through interactive manual tuning of the drive voltages whilst monitoring the frequency response, or by an automating search procedure to concentrate energy in the required frequency bands. In practice, it is helpful to first identify the voltage V_{i1} and V_{i0} for the most significant bit (i.e., $i = 3$) which shift the dominant peaks to the right or left of ~900Hz, respectively. A similar approach can then be used with the next bit (i.e., $i = 2$) and so on until all bits have been examined. Having achieved an initial estimate for the switch voltages, further tuning can then be performed to optimize the distribution and shape of the frequency peaks. Figure 4 shows the peaks observed for voltage settings found during calibration that correspond to OPDs $0,\ d_0, 7d_0$ and $15d_0$, respectively. However, there are several challenges that may need to be addressed. In our initial tests we have observed that the switch voltages exhibit poor repeatability, with the values drifting over time. We have addressed potential bulk temperature effects by mounting the PIC on a temperature-controlled platform, however, local temperature effects around the heaters may be influencing the switch voltages. The integrity of the mechanical contact between the electrical probe needles and the small pads on the PIC surface may also be a contributing factor. There is also potential for cross-talk between adjacent switches, where the heater introduces unwanted phase change in neighboring waveguides.

Having calibrated the ADL switches, the next step is to use another ADL on the die with an object beam terminated at a cleaved edge, coupled to an external GRIN lens and a retroreflector which distance to the lens can be changed, to demonstrate the principle of the active ADL in FSI for absolute distance measurements.

Downloaded From: https://www.spiedigitallibrary.org/conference-proceedings-of-spie on 08 Sep 2023
Terms of Use: https://www.spiedigitallibrary.org/terms-of-use

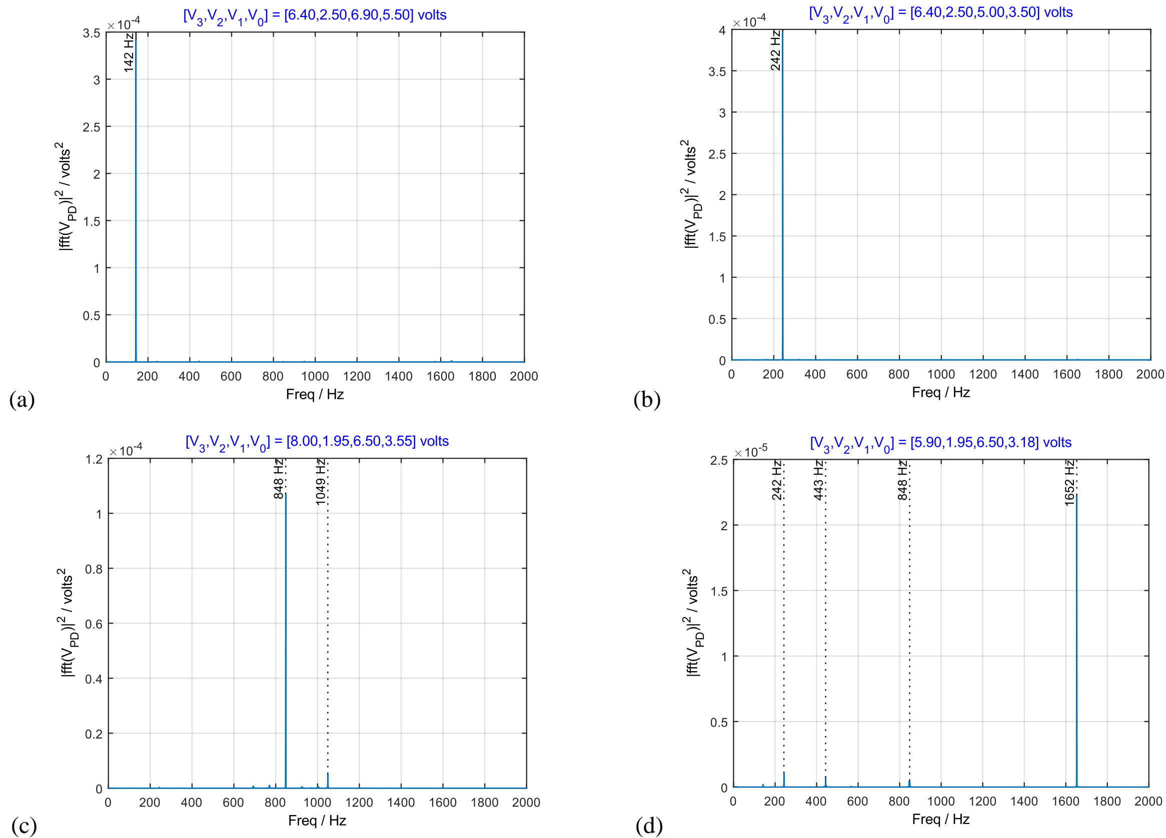

Figure 4. Frequency response observed when pre-calibrated voltages are applied to the switches. a-d) The binary state $[S_3, S_2, S_1, S_0]$ of the switches correspond to $[0, 0, 0, 0]$, $[0, 0, 0, 1]$, $[0, 1, 1, 1]$ and $[1, 1, 1, 1]$, which introduce OPDs 0, d_0, $7d_0$ and $15d_0$ respectively.

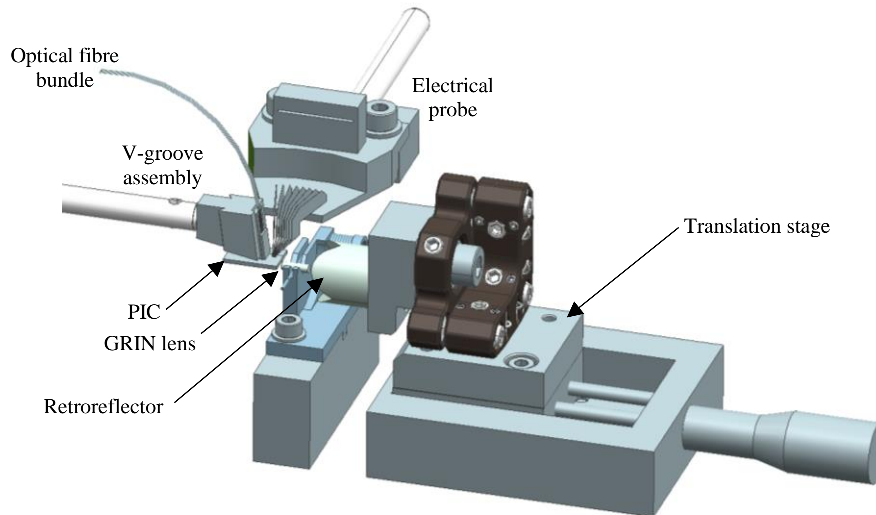

Figure 5: Annotated CAD render of an absolute distance measurement test rig based on a replicated hollow metal retroreflector, allowing the object beam path length to be precisely controlled over a range of ~40mm.

Switchable adaptive delay lines could enable FSI for large volume metrology in a cost-effective way, providing $\sim 10^5$ coordinates s^{-1} for ranges ~ 10 m and without requiring prohibitively expensive high-speed (>200GS/s) DAQ boards.

Downloaded From: https://www.spiedigitallibrary.org/conference-proceedings-of-spie on 08 Sep 2023
Terms of Use: https://www.spiedigitallibrary.org/terms-of-use

Limited by the sampling rate, every extra switch doubles the range or the maximum permissible sweep rate, and halves the coherence length requirement (an ADL with N switches relaxes coherence length requirements by a factor of 2^N). The delays in the ADL can be calibrated regularly, e.g. using a gas cell, at a frequency that should be higher than the expected thermal changes. We demonstrated the ADL concept for FSI ranging in [1, 2] using bulk optics, and here we presented the calibration of the optical switches of an ADL on a PIC, in a proof-of-principle device with a total range of tens of mm. Longer spiral waveguides have been demonstrated with over 20 m of physical path length [13], which would allow ADLs for range measurement of several meters, e.g. for aerospace applications such as wing and box-wing assembly dimensional metrology in the production line. Other silicon photonic platforms have potential advantages, e.g. Si_3N_4 offers lower propagation loss and greater thermal stability, even though coupling losses are high with grating couplers. Moreover, ADLs can be designed for the C-band (around 1550 nm) with the advantage of using higher laser powers while maintaining class I laser system classification. This would enable range measurement of diffuse surfaces (e.g. machined metal, composites, painted parts) without requiring sphere mounted retroreflectors or special reflective markers.

5. ACKNOWLEDGEMENTS

The authors gratefully acknowledge financial support from the Engineering and Physical Sciences Research Council to the Future Metrology Hub (EP/P006930/1) and CORNERSTONE (EP/L021129/1) projects, and from the Midlands Innovation Commercialisation of Research Accelerator (MICRA) and the Enterprise Project Group from Loughborough University (EPG 134-P5 1623). We are also grateful to Renishaw PLC for valuable technical discussions.

REFERENCES

1. C. A. Pallikarakis, J. M. Huntley, and P. D. Ruiz, “Adaptive delay lines for absolute distance measurements in high-speed long-range Frequency Scanning Interferometry,” OSA Contin, 4, 428–436 (2021).
2. C. A. Pallikarakis, J. M. Huntley, and P. D. Ruiz, “High-speed range and velocity measurement using frequency scanning interferometry with adaptive delay lines [Invited],” JOSA A, 37, 1814–1825 (2020).
3. R. Schödel, ed., “Modern Interferometry for Length Metrology,” (IOP Publishing, 2018).
4. M. C. Amann, T. Bosch, M. Lescure, R. Myllylä, and M. Rioux, “Laser ranging: a critical review of usual techniques for distance measurement,” Opt. Eng. 40, 10–19 (2001).
5. P. A. Coe, D. F. Howell, and R. B. Nickerson, “Frequency scanning interferometry in ATLAS: remote, multiple, simultaneous and precise distance measurements in a hostile environment,” Meas. Sci. Technol. 15, 2175–2187 (2004).
6. M. Takeda and H. Yamamoto, “Fourier-transform speckle profilometry: three-dimensional shape measurements of diffuse objects with large height steps and/or spatially isolated surfaces,” Appl. Opt. 33, 7829–7837 (1994).
7. A. Yamamoto, C.-C. Kuo, K. Sunouchi, S. Wada, I. Yamaguchi, and H. Tashiro, “Surface shape measurement by wavelength scanning interferometry using an electronically tuned Ti:sapphire laser,” Opt. Rev. 8, 59–63 (2001).
8. P. D. Ruiz, Y. Zhou, J. M. Huntley, and R. D. Wildman, “Depth-resolved whole-field displacement measurement using wavelength scanning interferometry,” J. Opt. A: Pure Appl. Opt. 6, 679–683 (2004).
9. A. Davila, J. M. Huntley, C. Pallikarakis, P. D. Ruiz, and J. M. Coupland, “Wavelength scanning interferometry using a Ti:Sapphire laser with wide tuning range,” Optics and Lasers in Engineering 50, 1089–1096 (2012).
10. J. Dale, B. Hughes, A. J. Lancaster, A. J. Lewis, A. J. H. Reichold, and M. S. Warden, “Multi-channel absolute distance measurement system with sub-PPM accuracy and 20 m range using frequency scanning interferometry and gas absorption cells,” Opt. Express 22, 24869–24893 (2014).
11. “CORNERSTONE,” https://www.cornerstone.sotonfab.co.uk/.
12. “EUROPRACTICE IC Service,” https://europractice-ic.com/.
13. H. Lee, T. Chen, J. Li, O. Painter and K. J. Vahala, “Ultra-low-loss optical delay line on a silicon chip,” Nat Commun, 3, 867-873 (2012).

Downloaded From: https://www.spiedigitallibrary.org/conference-proceedings-of-spie on 08 Sep 2023
Terms of Use: https://www.spiedigitallibrary.org/terms-of-use